Palladium-Catalyzed C-C Bond Activation and Regioselective Alkenylation between Cyclopropanol and 1,3-Diyne: One-Step Synthesis of Diverse Conjugated Enynes

Bedadyuti Vedvyas Pati, Asit Ghosh, Komal Yadav, Shyam Kumar Banjare, Upakarasamy Lourderaj* and P. C. Ravikumar*

School of Chemical Sciences, National Institute of Science Education and Research (NISER) Bhubaneswar, HBNI, Jatani, Khurda, 752050 Odisha, India

KEYWORDS C-C activation, conjugated enynes, regioselective alkenylation, cyclopropanol, 1,3-diynes

ABSTRACT: We report here the first example of the use of 1,3-dialkynes in C-C bond activation with any metal. The regio- and stereo-selective synthesis of 1,3-enynes from 1,3-diynes is demonstrated by the palladium-catalyzed C-C bond activation of cyclopropanol. Exclusive formation of mono-alkenylated adduct was achieved by eliminating the possibility of di-functionalization with high regio- and stereo-selectivity. Indeed, this protocol worked very well with electronically and sterically diverse substrates. Several studies, including deuterium labeling experiments and intermolecular competitive experiments, were carried out to understand the mechanistic details. The atomic-level mechanism followed in the catalytic process was also validated using DFT calculations, and the rate-controlling states in the catalytic cycle were identified. Further, preliminary mechanistic investigations with radical scavengers revealed non-involvement of the radical pathway for this transformation.

Transition metal-catalyzed selective activation of C-H and C-C bonds have gained enormous significance in recent years owing to their potential application in chemical transformations.[1, 2] Especially, the strategy involving selective cleavage of C-H bond followed by subsequent insertion of 2π-unsaturated unit has been recognized as one of the most attractive approaches to access diverse molecular entities from the readily available feedstock.[3] This strategy also helps in building rapid complexity following the high atom-economical process. In this context, the one-step synthesis of conjugated 1,3-enynes through this process is of great importance due to their vast abundance in various natural products and pharmaceuticals (Scheme 1).[4]

Scheme 1. Representative examples of natural products and drug molecules bearing conjugated 1,3-enyne scaffold

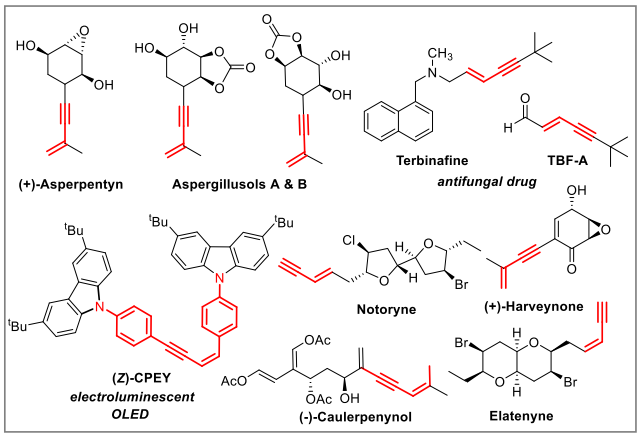

Consequently, they have been well recognized as multifaceted building units in organic synthesis.[5] Moreover, these structural units also receive considerable interest in material sciences and medicinal chemistry.[6]

Considering their profound synthetic usefulness, 1,3-diynes have been recently introduced as a coupling partner for transition-metal catalyzed reactions to access conjugated 1,3-enynes.[7] Nevertheless, the use of 1,3-diynes in these reactions is always associated with particular challenges. The most commonly faced challenges are: (a) difficulty in controlling stereo- and regio-selectivity and (b) difficulty in controlling mono-functionalization over di-functionalization.[3b, 7] As a result, only a few protocols for the synthesis of 1,3-enynes using 1,3-diynes have been described to date.[7] Ge and co-workers developed a cobalt-catalyzed regiodivergent and stereoselective hydroboration of 1,3-diynes to afford boryl-functionalized enynes (Scheme-2a(i)).[7a] In another report, Beller and co-workers also disclosed palladium-catalyzed selective synthesis of conjugated enynes employing alkoxycarbonylation of 1,3-diynes (Scheme-2a(ii)).[7b] Interestingly, highly selective synthesis of 1,3-enynes has also been achieved by Glorius and co-workers via manganese-catalyzed C-H activation-alkenylation of arenes and heteroarenes with 1,3-diynes (Scheme-2a(iii)).[7c] Because of the challenges mentioned above, reports on using 1,3-diynes to synthesize conjugated enynes are minimal. Indeed, the possibility of C-C bond activation and alkenylation sequence for 1,3-dynes has never been attempted.

In this context, the tandem activation and functionalization of the C-C bond is quite challenging. It is mainly due to the following reasons: (i) poor accessibility of C-C bonds by the catalyst as compared to C-H bonds, (ii) greater thermodynamic barrier to break a stronger C-C bond, and (iii) poor orbital

Scheme 2. Use of 1,3- diynes to access conjugated enynes. (a) previous report, (b) this work.

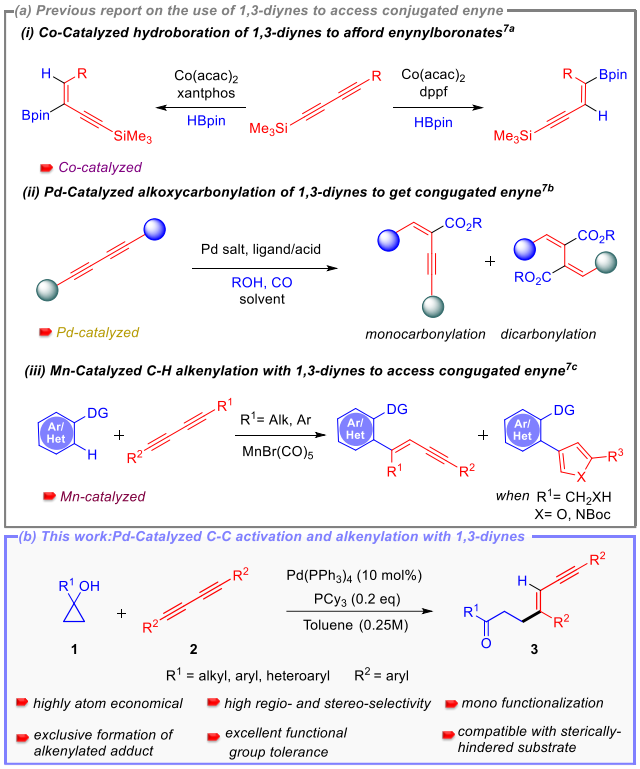

directionality of C-C bonds makes it less favorable compared to C-H bonds for effective interactions with transition metal complexes. Despite these difficulties, substantial efforts have been made over the last two decades to activate different types of C-C bonds.[2, 8] Some valuable strategies employed include *β*-carbon elimination, [8a, c] oxidative addition, [2d] and aromatization driven processes.[8d] In this regard, one of the recent and attractive processes includes the C-C bond activation of small rings by taking advantage of their intrinsic ring strain.[9] The thermodynamic barrier is largely offset with the aid of release in ring strain. The synthetic potential of this method has been successfully demonstrated by several research groups such as Dong, Jun, Murakami, Bower, Yu, Loh, and Marek to access an array of useful structural motifs.[10] Cyclopropanol obtained from Kulinkovich protocol is one of the smallest ring molecules whose ring strain has been exploited to synthesize various molecular architectures.[11-13] Our group has also developed the strain-driven C-C bond activation of cyclopropanol and cyclopropenone to furnish diverse functionalized molecular units.[14]

Owing to the synthetic value of conjugated enynes and the significance of developing new methodology using 1,3-diynes, we envisioned that the strain-driven C-C bond activation-subsequent alkenylation of cyclopropanol would effectively result in the formation of the desired 1,3-enynes. Herein, we report a palladium-catalyzed C-C bond activation and regio-and stereo-selective mono-alkenylation of readily accessible cyclopropanol to synthesize divergent 1,3-enynes rapidly (Scheme-2b).

To establish our methodology, we started with identifying the suitable reaction conditions for the palladium-catalyzed C-C bond activation of cyclopropanol and the subsequent alkenylation with 1,3-diyne. Subsequently, 1-benzylcyclopropan-1-ol **1a** and 1,4-diphenylbuta-1,3-diyne **2a** were chosen as the model substrates in the presence of 10 mol % of a palladium catalyst. Initially, different palladium catalysts were screened in the absence of ligand in toluene at 100 °C

Table 1. Optimization of Reaction Conditions[a]

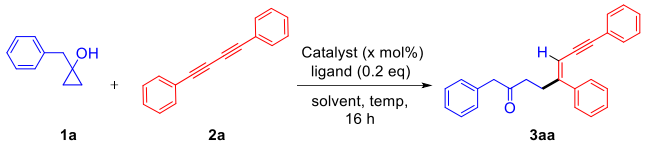

entry	catalyst	ligand	solvent	temp (°C)	yield[b]
1	$PdCl_2$	-	Toluene	100	nd[c]
2	$PdCl_2(PPh_3)_2$	-	Toluene	100	nd[c]
3	$Pd(dba)_2$	-	Toluene	100	19
4	$Pd(OCOCF_3)_2$	-	Toluene	100	nd[c]
5	$Pd(PPh_3)_4$	-	Toluene	100	56
6	$Pd(PPh_3)_4$	-	THF	100	40
7	$Pd(PPh_3)_4$	-	MeCN	100	29
8	$Pd(PPh_3)_4$	-	DMF	100	25
9	$Pd(PPh_3)_4$	-	Toluene	80	34
10	$Pd(PPh_3)_4$	-	Toluene	120	42
11[d]	$Pd(PPh_3)_4$	-	Toluene	100	69
12[d]	$Pd(PPh_3)_4$	PPh_3	Toluene	100	53
13[d]	$Pd(PPh_3)_4$	RuPhos	Toluene	100	62
14[d]	$Pd(PPh_3)_4$	$P(^tBu)_3.HBF_4$	Toluene	100	77
15[d]	**$Pd(PPh_3)_4$**	**PCy_3**	**Toluene**	**100**	**89(86)**
16[d]	$Pd(PPh_3)_4$	$PCy_3.HBF_4$	Toluene	100	68
17[d, e]	$Pd(PPh_3)_4$	PCy_3	Toluene	100	73
18[d, f]	$Pd(PPh_3)_4$	PCy_3	Toluene	100	77
19[d]	-	PCy_3	Toluene	100	nd[c]

[a]Unless otherwise specified, all reactions were carried out using catalyst (10 mol %), ligand (0.2 equiv), **1a** (0.10 mmol, 1.0 equiv), **2a** (0.10 mmol, 1.0 equiv) in a solvent (0.25 M) for 16 h. [b]Yields determined by NMR, using 1,3,5-trimethoxy benzene as internal reference. [c]nd = not detected. [d]Using **1a** (0.20 mmol, 2.0 equiv) and 2a (0.10 mmol, 1.0 equiv) while the other conditions remained the same. [e]Using catalyst (5 mol %) while the other conditions remained the same. [f]Using catalyst (10 mol %) and ligand (0.1 equiv) while the other conditions remained the same. Isolated yield is mentioned in the parenthesis.

(Table 1, entries 1-5). The desired alkenylated adduct **3aa** was obtained in 19% and 56% yields with $Pd(dba)_2$ and $Pd(PPh_3)_4$ respectively (Table 1, entries 3 and 5). Other palladium catalysts such as $PdCl_2$, $PdCl_2(PPh_3)_2$, and $Pd(OCOCF_3)_2$ remained ineffective (Table 1, entries 1, 2 and 4). The use of other solvents such as tetrahydrofuran, acetonitrile, and dimethylformamide, with $Pd(PPh_3)_4$ as the catalyst, did not

improve the product yield (Table 1, entries 6-8). Increasing or decreasing the reaction temperature (120 °C and 80 °C) had a deleterious effect on the reaction furnishing the desired product **3aa** in 34% and 42% yields, respectively (Table 1, entries 9 and 10). Hence, we chose $Pd(PPh_3)_4$ as the catalyst in toluene at 100 °C and varied the other reaction parameters. It is worth mentioning here that the reactive metal-homoenolate generated after the *β*-carbon elimination from **1a** may undergo protodemetalation to give a ring-opened isomerized product resulting in significant loss of the product yield. Therefore, we increased the equivalence of **1a**. To our delight, 69% of **3aa** was obtained using 2 equivalents of **1a** (Table 1, entry 11). Next, we investigated the effect of different phosphine ligands (Table 1, entries 12-16). Gratifyingly, the yield of **3aa** further improved in the cases of $P(^tBu)_3.HBF_4$ (77%) and PCy_3 (89%). (Table 1, entries 14, 15). Further, variation in molar percentage of $Pd(PPh_3)_4$ and PCy_3 did not enhance the product yield (Table 1, entries 17, 18 and 19). We then performed a control experiment without $Pd(PPh_3)_4$ catalyst. As expected, it did not produce the product, thus, confirming the key role of catalyst in this reaction (entry 20). Hence, the use of 10 mol % of $Pd(PPh_3)_4$, 0.2 equivalent of PCy_3 in toluene (0.25 M) at 100 °C is the best optimized condition for the synthesis of **3aa** (Table 1, entry 15).

Having established the optimized reaction conditions, we next moved to assess the robustness of this highly regio- and stereo-selective alkenylation of cyclopropanols (Table 2). To showcase the diversity of this protocol, we subjected various benzyl-, alkyl-, aryl-, heteroaryl-substituted cyclopropanol **1** and aryl-substituted 1,3-diynes **2** to the standard reaction conditions. Initially, we examined the feasibility of different benzyl-substituted cyclopropanols. Cyclopropanols bearing electron-donating as well as withdrawing benzyl substituents worked efficiently, furnishing 63-86% yield of their respective alkenylated adducts **3aa**-**3ea**. Furthermore, we also found the alkenylation reaction viable with disubstituted cyclopropanols afforded their respective adducts **3fa** and **3ga** in 91% and 50% yields respectively. It is worth mentioning that various alkyl (linear-chain and alicyclic) substituted cyclopropanols as well as sterically hindered cyclopropanol **1i** reacted smoothly to produce the desired alkenylated adducts **3ha**-**3ma** in 64-80%

Table 2. Scope of cyclopropanols and 1,3-diynes for the synthesis of conjugated enynes[a]

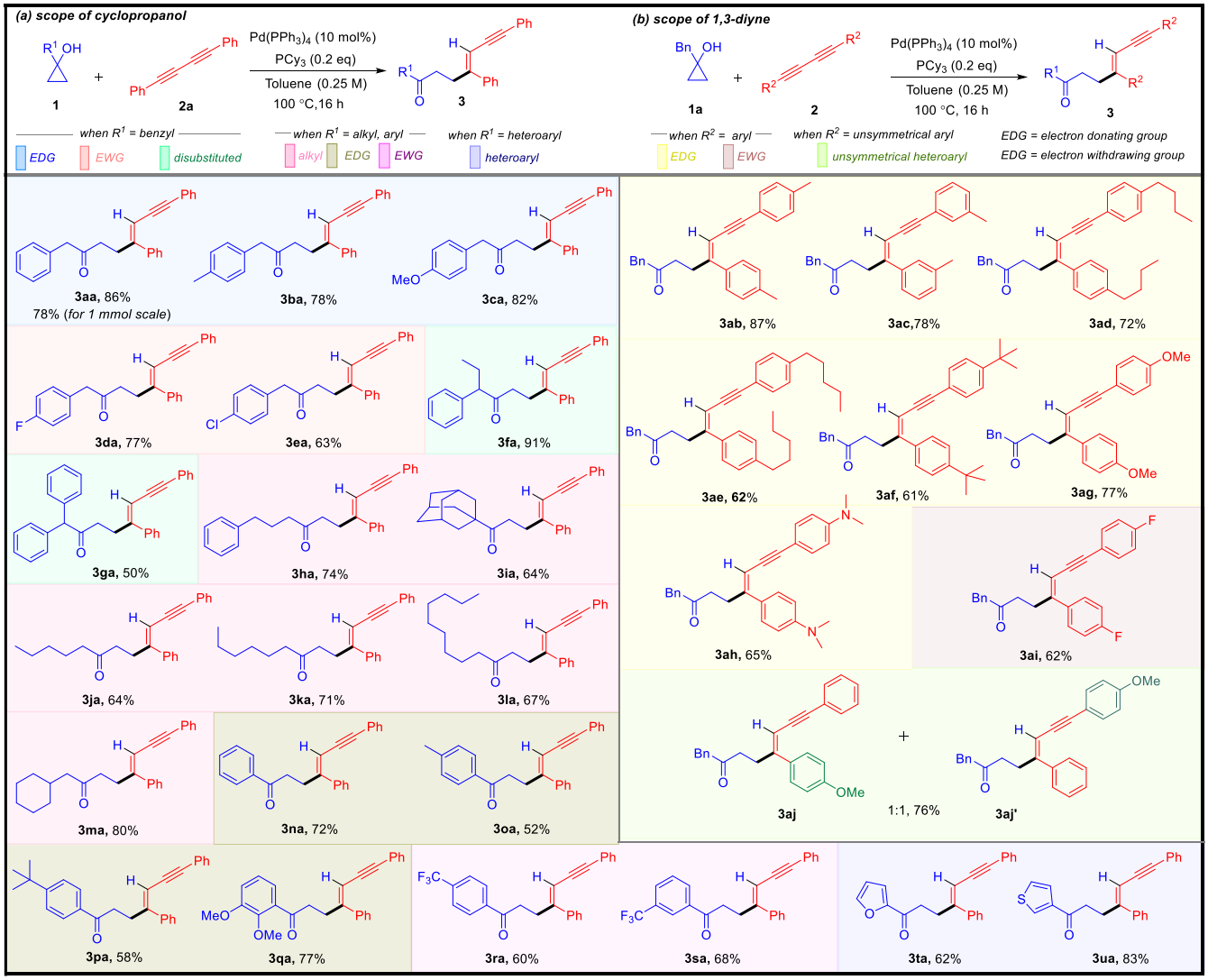

[a]All reactions were carried out using $Pd(PPh_3)_4$ (10 mol %), PCy_3 (0.2 equiv), **1** (0.20 mmol, 2.0 equiv), **2** (0.10 mmol, 1.0 equiv) in toluene (0.25 M) at 100 °C for 16 h.

yield. After successfully demonstrating the scope of alkenylation with benzyl- and alkyl-substituted cyclopropanols, we focused our attention on unraveling the scope of different aryl- and heteroaryl-substituted cyclopropanols. Similar to the benzyl-substituted cyclopropanols, both electronically-rich and electronically-poor aryl-substituted cyclopropanols were facile, resulting in good yields of their corresponding alkenylated adducts **3na**-**3ua**. Pleasingly, cyclopropanols bearing furan- and thiophene-substituents underwent the transformation efficiently, yielding **3ta** and **3ua** in 62% and 83% yield, respectively.

After successfully exploring the scope of structurally and electronically distinct cyclopropanols for the developed methodology, we further investigated the scope with different 1,3-diynes. Both electronically rich and poor 1,3- diynes furnished their corresponding alkenylated adduct **3ab**-**3aj** in 61-87% yields. The regio- and the stereo-selectivity of the product molecule was confirmed unambiguously from the NOE experiment of **3aa**. To test the synthetic practicality of the developed C-C activation protocol, we performed a 1 mmol scale reaction with **1a** and **2a** to produce **3aa** in 78% yield.

Scheme 3. Mechanistic Studies

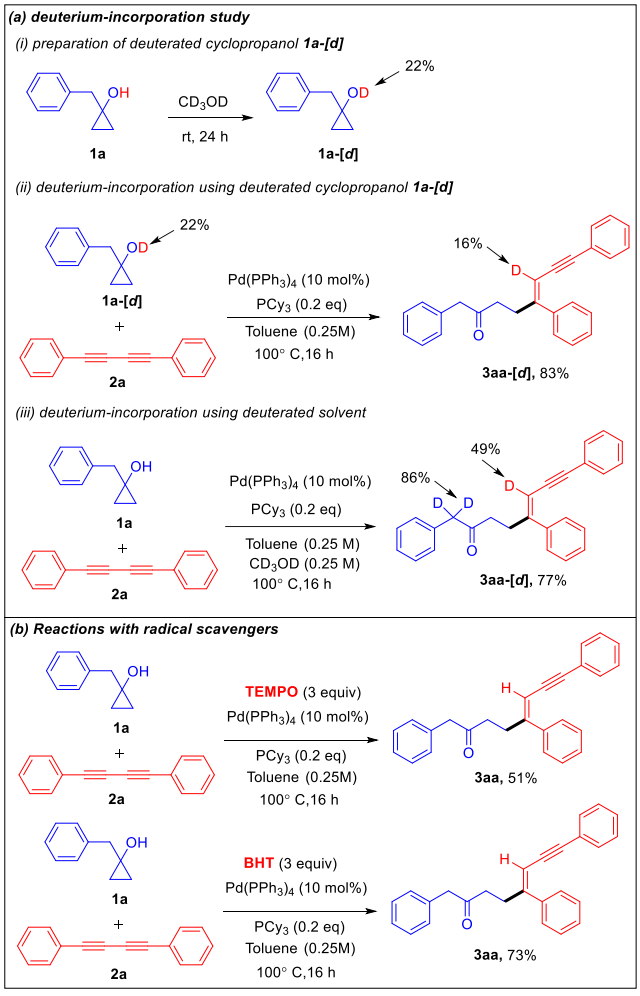

Encouraged by the versatility of the developed transformation, we performed a series of experiments to get insight on the mechanism of the catalytic cycle. Initially, we conducted a set of deuterium incorporation studies using deuterated substrate **1a-[*d*]** and deuterated solvent CD_3OD (Scheme-3a). The reaction of **1a-[*d*]** (22% D) and **2a** afforded the **3aa-[*d*]** in 83% yield with 16% deuteration at the olefinic proton (Scheme-3a-ii). When we used CD_3OD as a co-solvent, 49% deuteration at the olefinic proton and 86% deuteration at the benzylic proton of **3aa-[*d*]** was observed with 77% yield. To investigate the involvement of radical pathway, we carried out two reactions in the presence of radical scavengers such as 2,2,6,6-tetramethylpiperidine 1-oxyl (TEMPO) and 2,6-di-*tert*-butyl-4-methyl-phenol (BHT) (Scheme-3b). The **3aa** yields of 51% and 73% in the presence of TEMPO and BHT respectively refuted the possibility of a radical pathway.

Moreover, for further mechanistic insights we conducted two intermolecular competitive experiments. First, two electronically different cyclopropanols **1o** and **1t** were subjected to the standard reaction conditions with diyne **2a** that afforded **3oa**:**3ta** in 6.14:1 ratio (Scheme 4a). Next, the competitive experiment between two different diynes **2g** and **2i** with cyclopropanol **1a** afforded **3ag**:**3ai** in 1:1.84 ratio (Scheme 4b). These results reveal that alkenylation is more favorable for electronically rich cyclopropanols and electronically poor diynes.

Scheme 4. Competitive Experiments

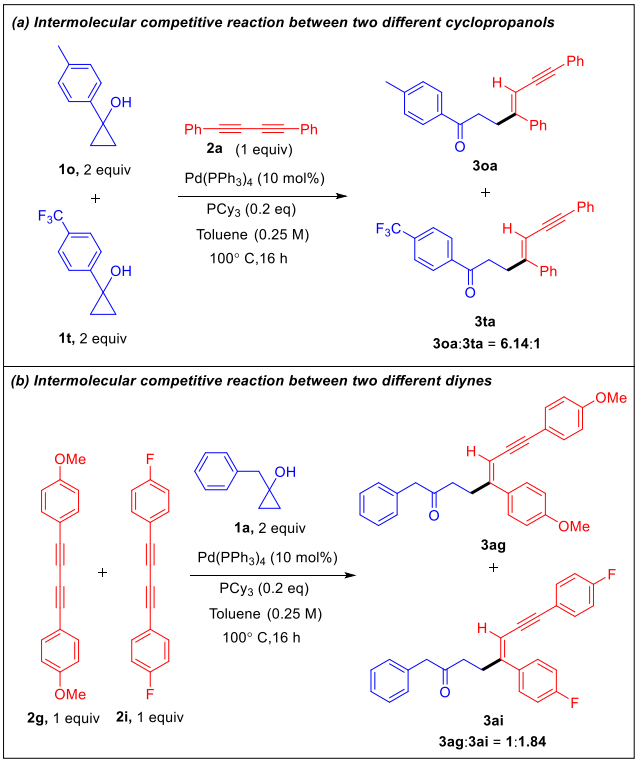

To understand the atomic-level mechanism followed in the reaction between **1a** and **2a** catalyzed by $Pd(PPh_3)_4$, we performed density functional theoretical (DFT) calculations using the B3LYP[15-16] functional with 6-31G(d,p)[17] basis sets, with the LANL2DZ[18] pseudopotential to represent the core electrons of Pd. We performed all calculations in the presence of toluene as the solvent using the SMD[19] solvation model and mapped the (Gibbs) free energy profile along the reaction path. The free energies were calculated at the experimental temperature of 373.15 K. See the supporting information for a detailed description of the methods used in the calculations.

In cross-coupling reactions involving Pd catalysts, PdL_4 dissociates to PdL_3, which is in equilibrium with PdL_2.[20] The PdL_2 has been observed to behave as the active species and thus

controls the oxidative addition step. Hence, in the DFT calculations, we have considered $Pd(PPh_3)_2$ as the active catalyst while computing the energy profile for the reaction. Figure 1 gives the complete free energy profile for the reaction path involving various stationary points. The molecular structures of the stationary points and the important geometrical parameters are given in Figure S1 in the supporting information.

The catalytic reaction cycle begins with the approach of the active catalyst $Pd(PPh_3)_2$ and **1a** towards each other to form the complex **int1** having an energy of 16.36 kcal/mol with the H atom of the OH group of **1a** pointing towards Pd (H-Pd distance = 2.46 Å). The next step is the oxidative addition of the alcoholic -OH group to the Pd center to result in **int2**. The oxidative addition is achieved by the concerted dissociation of the O-H bond and the formation of Pd-O and Pd-H coordinate bonds via a three-membered cyclic transition state **ts1** with a barrier of 42.82 kcal/mol. In **int2**, the Pd center is tetracoordinated with Pd-O (2.06 Å) and Pd-H (1.55 Å) bonds and takes a square planar geometry. Then, the addition of H (hydrogenation of) to the C≡C bond takes place. For this to happen, first, an elimination of PPh_3 from **int2** results in **int3**, which is crucial to lower steric hindrance and accommodate the incoming **2a**. This step is followed by the approach of **2a** towards **int3** to give the intermediate **int4**. It should be noted that the free rotation of the O-C bond in the intermediates (**int1**, **int2**, and **int3**) leads to the formation of different conformational isomers. However, the energy differences between the conformational isomers were less than 1 kcal/mol.

What ensues is the hydrogenation of the unsaturated alkyne bond by the *syn* addition of Pd-H to the C≡C bond to form the intermediate **int5**. This is a concerted step via a four-membered cyclic transition state **ts2** with a barrier of 12.9 kcal/mol. In going from **int4** to **ts2**, the hydrogen atom of the Pd-H bond is stretched, and the C≡C bond is aligned coplanar to the square planar orientation of the Pd center to facilitate the H···C≡C interaction. From **ts2**, the H migration results in **int5** with the Pd center maintaining a planar geometry. The intermediate **int5** then undergoes β-carbon elimination to form **int6**. During this process, the Pd-C_β bond is formed accompanied by the simultaneous breaking of the C_α-C_β and O-Pd bonds via a four-membered cyclic transition state **ts3** with a barrier of 1.0 kcal/mol. Now, the addition of a PPh_3 group to **int6** leads to the

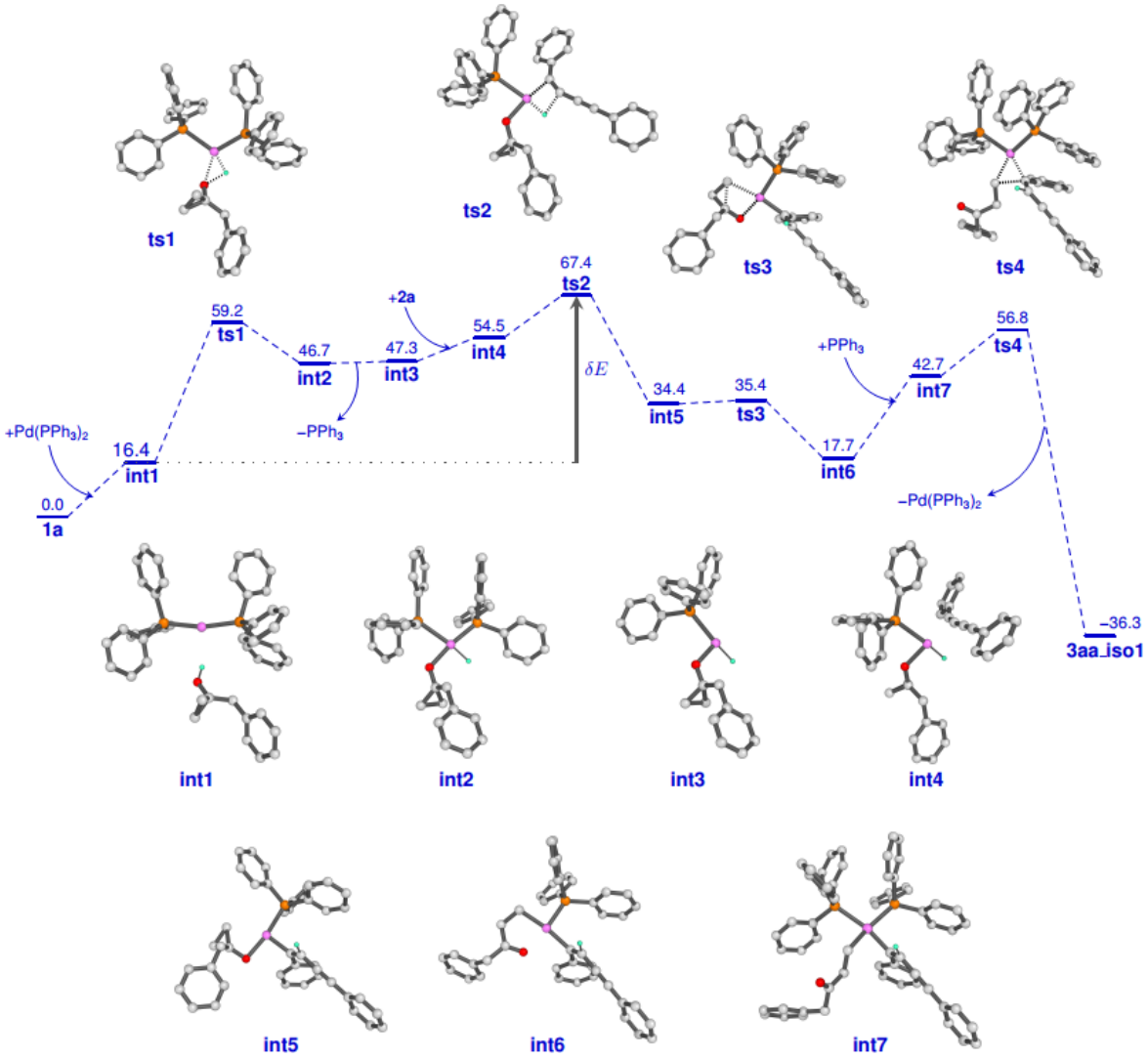

Figure 1. Free energy profile for the reaction between **1a** and **2a** catalyzed by $Pd(PPh_3)_2$, calculated at the B3LYP/6-31G(d,p) level of theory. The energies (kcal/mol) are reported with respect to **1a** + **2a** + $Pd(PPh_3)_2$. The effective free energy barrier (*dE*) for the reaction is shown as dark gray arrow.

formation of the intermediate **int7** with a *tetra*-coordinated Pd center. The final step in the cycle is the reductive elimination process at the Pd center from **int7** to the product **3aa_iso1**. Here, the two Pd-C bonds in **int7** are broken with the concomitant bond formation between the associated carbon atoms via a cyclic three-membered transition state **ts4** with a 14.0 kcal/mol barrier. The product **3aa_iso1** is stabilized by -36.33 kcal/mol with respect to the reactants. The product **3aa_iso1** can exist in different isomeric forms (**3aa_iso2**, **3aa_iso3**, **3aa_iso4**, and **3aa_iso5**) due to rotation about C-C sigma bonds that are within 2 kcal/mol in energies. In addition, the *β*-carbon elimination can happen for alternative isomers of **int5** to result in isomeric products. For example, *β*-carbon elimination from **int5′**followed by reductive elimination at the Pd center results in the product **3aa_iso2** (Figure S4). However, as pointed above, the different isomers are within 2 kcal/mol, and the overall reaction pathways follow similar steps.

It is of interest to identify the rate-controlling states involved in the overall reaction. To this end, we computed the turnover frequency (TOF) for the reaction using the energetic span model.[21] From the energetics of the reaction, we can see that the TOF determining transition state (TDTS) and the TOF determining intermediate (TDI) are **ts2** and **int1**, respectively. Hence, the effective free energy barrier (δE) for the catalytic cycle is 42.8 kcal/mol, as noted in the energy profile (Figure 1).

In accordance to the aforementioned mechanistic outcomes from experiments supported by DFT calculations at the B3LYP/6-31G(d,p) level of theory and literature precedents,[11] a plausible catalytic cycle is depicted in Scheme 5. The catalytic cycle starts with the oxidative addition of cyclopropanol **1a** to active $PdL_2(0)$ catalyst to form the intermediate **int2**. The intermediate **int2** then undergoes π-coordination with 1,3-diyne **2a** to afford intermediate **int4**, which undergoes *syn* addition and hydrogen atom transfer to furnish intermediate **int5**. *β*-Carbon elimination from the intermediate **int5** then leads to the formation of palladium homoenolate intermediate **int7**. Finally, the reductive elimination from palladium homoenolate intermediate **int7** results in the alkenylated adduct **3aa** with the regeneration of Pd(0) catalyst.

Scheme 5. Proposed Catalytic Cycle

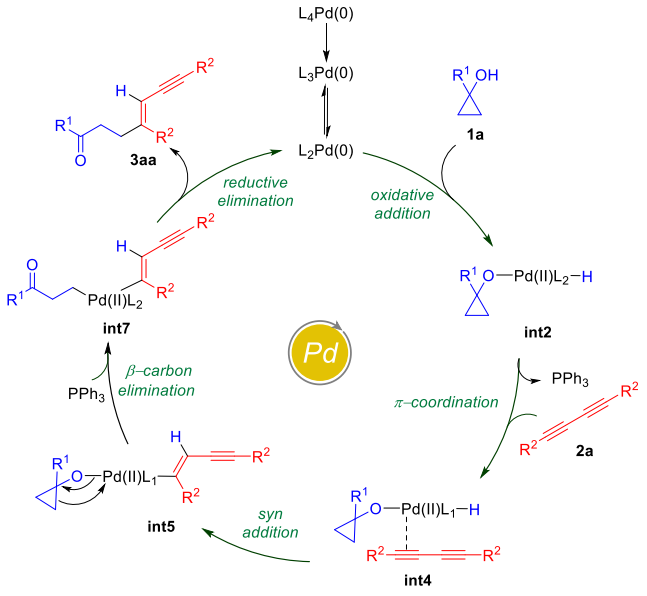

In conclusion, we have developed a palladium-catalyzed novel and highly regio/stereo-selective synthetic strategy to get an array of 1,3-enyne derivatives via C-C activation of cyclopropanol followed by alkenylation with 1,3-diynes. Apart from high regio- and stereo-selectivity, excellent functional group tolerance has also been achieved with both the cyclopropanol and 1,3-diynes. The protocol was found to be amenable to sterically hindered cyclopropanols such as adamantane cyclopropanol. Importantly, eliminating the possibility of difunctionalization, exclusive mono-functionalization has also been achieved. Several mechanistic investigations including deuterium labelling experiments have been carried out. In addition, the reaction mechanism of the catalytic process was supported using DFT calculations and it was found that the step corresponding to the hydrogenation of the alkyne bond acted as the rate-controlling step for the reaction. The preliminary mechanistic findings with radical scavengers revealed non-involvement of the radical pathway for the transformation.

ASSOCIATED CONTENT

Supporting Information. Experimental details and characterization data of the compounds. This material is available free of charge via Internet at http://pubs.acs.org.

AUTHOR INFORMATION

Corresponding Author

* Email: pcr@niser.ac.in, and u.lourderaj@niser.ac.in.

Author Contributions

The manuscript was written through the contributions of all authors. / All authors have approved the final version of the manuscript.

Notes

The authors declare no competing financial interest.

ACKNOWLEDGMENT

We acknowledge DAE, Govt. of India, Council for Scientific and Industrial Research (CSIR), New Delhi (Grant 02(0256)/16/EMR II), and the Science and Engineering Research Board (SERB), New Delhi (Grant EMRII/2017/001475) for financial support. B.V.P. thanks DST-INSPIRE, A.G. and K.Y. and S.K.B thank DAE for research fellowship.

REFERENCES

(1) For selected recent reviews on transition-metal-catalyzed C−H activation: (a) Wencel-Delord, J.; Glorius, F. C-H Bond Activation Enables the Rapid Construction and Late-Stage Diversification of Functional Molecules. *Nat. Chem.* **2013**, *5*, 369−375. (b) Rouquet, G.; Chatani, N. Catalytic Functionalization of C(sp2)-H and C(sp3)-H Bonds by Using Bidentate Directing Groups. *Angew. Chem., Int. Ed.* **2013**, *52*, 11726−11743. (c) Thirunavukkarasu, V. S.; Kozhushkov, S. I.; Ackermann, L. C-H Nitrogenation and Oxygenation by Ruthenium Catalysis. *Chem. Commun*. **2014**, *50*, 29−39. (d) Moselage, M.; Li, J.; Ackermann, L. Cobalt-Catalyzed C-H Activation. *ACS Catal*. **2016**, *6*, 498−525. (e) Hummel, J. R.; Boerth, J. A.; Ellman, J. A. Transition Metal-Catalyzed C-H Bond Addition to Carbonyls, Imines, and Related Polarized *π*- Bonds. *Chem. Rev.* **2017**, *117*, 9163−9227. (f) Sambiagio, C.; SchÖnbauer, D.; Blieck, R.; DaoHuy, T.; Pototschnig, G.; Schaaf, P.; Wiesinger, T.; Zia, M. F.; WencelDelord, J.; Besset, T.; Maes, B. U. W.; Schnürch, M. A comprehensive overview of directing groups applied in metal-catalysed C−H functionalisation chemistry. *Chem. Soc. Rev.* **2018**, *47*, 6603−6743. (g) Gandeepan, P.; Müller, T.; Zell, D.; Cera, G.; Warratz, S.; Ackermann, L. 3d Transition Metals for

C-H Activation. *Chem. Rev.* **2019**, *119*, 2192−2452. (h) Dutta, U.; Maiti, S.; Bhattacharya, T.; Maiti, D. Arene diversification through distal C(sp^2)−H functionalization. *Science*. **2021**, *372*, No. eabd5992 and the references cited therein.

(2) For selected recent reviews on transition metal-catalyzed C-C activation: (a) Murakami, M.; Matsuda, T. Metal-Catalysed Cleavage of Carbon Carbon Bonds. *Chem. Commun.* **2011**, *47*, 1100−1105. (b) Ruhland, K. Transition Metal-Mediated Cleavage and Activation of C-C Single Bonds. *Eur. J. Org. Chem.* **2012**, *2012*, 2683−2706. (c) Chen, F.; Wang, T.; Jiao, N. Recent Advances in Transition Metal-Catalyzed Functionalization of Unstrained Carbon-Carbon Bonds. *Chem. Rev.* **2014**, *114*, 8613−8661. (d) Souillart, L.; Cramer, N. Catalytic C-C Bond Activations via Oxidative Addition to Transition Metals. *Chem. Rev*. **2015**, *115*, 9410−9464. (e) Murakami, M.; Ishida, N. Potential of Metal-Catalyzed C−C Single Bond Cleavage for Organic Synthesis. *J. Am. Chem. Soc*. **2016**, *138*, 13759−13769. (f) Chen, P. H.; Billett, B. A.; Tsukamoto, T.; Dong, G. ″Cut and Sew″ Transformations via Transition-Metal-Catalyzed Carbon−Carbon Bond Activation. *ACS Catal*. **2017**, *7*, 1340−1360. (g) Song, F.; Gou, T.; Wang, B. Q.; Shi, Z. J. Catalytic Activations of Unstrained C−C Bond Involving Organometallic Intermediates. *Chem. Soc. Rev*. **2018**, *47*, 7078−7115. (h) McDonald, T. R.; Mills, L. R.; West, M. S.; Rousseaux, S. A. L. Selective Carbon−Carbon Bond Cleavage of Cyclopropanols. *Chem. Rev.* **2021**, *121*, 3−79 and references cited therein.

(3) (a) Zhang, W.; Li, H.; Wang, L. Cobalt-Catalyzed Temperature-Dependent Annulation of 3- Aryl- 1,2,4-oxadiazolones with 1,3-Diynes: An Approach to π-Conjugated Molecules. *Adv. Synth. Catal.* **2019**, *361*, 2885−2896. (b) Yu, D.-G.; De Azambuja, F.; Gensch, T.; Daniliuc, C. G.; Glorius, F. The C−H Activation/1,3-Diyne Strategy: Highly Selective Direct Synthesis of Diverse Bisheterocycles by Rh(III) Catalysis. *Angew. Chem., Int. Ed.* **2014**, *53*, 9650−9654. (c) Kathiravan, S.; Nicholls, I. A. Cobalt Catalyzed, Regioselective C(sp^2)-H Activation of Amides with 1,3-Diynes. *Org. Lett*. **2017**, *19*, 4758−4761. (d) Sen, M.; Mandal, R.; Das, A.; Kalsi, D.; Sundararaju, B. Cp*Co(III)−Catalyzed Bis-isoquinolone Synthesis by C−H Annulation of Arylamide with 1,3-Diyne. *Chem. - Eur. J.* **2017**, *23*, 17454−17457. (e) Gao, Y.; Zeng, F.; Sun, X.; Zeng, M.; Yang, Z.; Huang, X.; Shen, G.; Tan, Y.; Feng, R.; Qi, C. One-pot Synthesis of Alkynylated Coumarins via Rhodium-Catalyzed Annulation of Aryl Thiocarbamates with 1,3-Diynes or Terminal Alkynes. Adv. Synth. Catal. **2018**, *360*, 1328−1333. (f) Martínez, Á. M.; Alonso, I.; Rodríguez, N.; Arrayas, R. G.; Carretero, J. C. Rhodium-Catalyzed Copper-Assisted Intermolecular Domino C−H Annulation of 1,3−Diynes with Picolinamides: Access to Pentacyclic π−Extended Systems. *Chem. - Eur. J.* **2019**, *25*, 5733−574. (g) Feng, R.; Ning, H.; Su, H.; Gao, Y.; Yin, H.; Wang, Y.; Yang, Z.; Qi, C. Selective Synthesis of Alkynylated Isoquinolines and Biisoquinolines via Rh(III) Catalyzed C−H Activation/1,3-Diyne Strategy. *J. Org. Chem*. **2017**, *82*, 10408−10417. (h) Mei, R.; Ma, W.; Zhang, Y.; Guo, X.; Ackermann, L. Cobaltaelectro-Catalyzed Oxidative C−H/N−H Activation with 1,3-Diynes by Electro-Removable Hydrazides. *Org. Lett.* **2019**, *21*, 6534−6538. (i) Qian, S.; Pu, X.; Chang, G.; Huang, Y.; Yang, Y. Rh(III)-Catalyzed oxidative C-H activation/domino annulation of anilines with 1,3-diynes: A rapid access to blue emitting tricyclic N,O-heteroaromatics. *Org. Lett*. **2020**, *22*, 5309−5313. (j) Dey, A.; Volla, C. M. R. Traceless Bidentate Directing Group Assisted Cobalt-Catalyzed sp^2 -C-H Activation and [4 + 2]-Annulation Reaction with 1,3-Diynes. *Org. Lett*. **2020**, *22*, 7480−7485. (k) Pati, B. V.; Sagara, P. S.; Ghosh, A.; Adhikari, GK. D.; Ravikumar, P. C. Ruthenium-Catalyzed Regioselective C(sp^2)–H Activation/Annulation of N-(7-Azaindole)amides with 1,3-Diynes Using N-Amino-7-azaindole as the N,N-Bidentate Directing Group. *J. Org. Chem*. **2021**, *86*, 9428–9443. (l) Zhao, F.; Gong, X.; Lu, Y.; Qiao, J.; Jia, X.; Ni, H.; Wu, X.; Zhang, X. Additive-Controlled Divergent Synthesis of Tetrasubstituted 1,3-Enynes and Alkynylated 3*H*-Pyrrolo[1,2-a]- indol-3-ones via Rhodium Catalysis. *Org. Lett*. **2021**, *23*, 727−733 and references cited therein.

(4) For selected examples, see: (a) Rudi, A.; Schleyer, M.; Kashman, Y. Clathculins A and B, Two Novel Nitrogen-Containing Metabolites from the Sponge Clathrina aff. Reticulum. *J. Nat. Prod.* **2000**, *63*, 1434-1436. (b) Iverson, S. L.; Uetrecht, J. P. Identification of a reactive metabolite of terbinafine: insights into terbinafine-induced hepatotoxicity. *Chem. Res. Toxicol.* **2001**, *14*, 175-181. (c) El-Jaber, N.; Estevez-Braun, A.; Ravelo, A. G.; Munˇoz- Munˇoz, O.; Rodriguez-Afonso, A.; Murguia, J. R. Acetylenic Acids from the Aerial Parts of Nanodea muscosa. *J. Nat. Prod*. **2003**, *66*, 722-724. (d) Furstner, A.; Turet, L. Concise and Practical Synthesis of Latrunculin Aby Ring-Closing Enyne–Yne Metathesis. *Angew. Chem., Int. Ed*. **2005**, *44*, 3462-3466.

(5) For selected reviews, see: (a) Bergman, R.G. Reactive 1,4-dehydroaromatics. *Acc. Chem. Res*. **1973**, *6*, 25–31. (b) Saito, S.; Yamamoto, Y. Recent Advances in the Transition-Metal-Catalyzed Regioselective Approaches to Polysubstituted Benzene Derivatives. *Chem. Rev*. **2000**, *100*, 2901–2916. (c) Chinchilla, R.; Njera, C. Chemicals from Alkynes with Palladium Catalysts. *Chem. Rev*. **2014**, *114*, 1783–1826. (d) Holmes, M.; Schwartz, L. A.; Krische, M. J. Intermolecular MetalCatalyzed Reductive Coupling of Dienes, Allenes, and Enynes with Carbonyl Compounds and Imines. *Chem. Rev*. **2018**, *118*, 6026−6052. (e) Xiao, Y.; Zhang, J. Tetrasubstituted furans by a Pd(II)-catalyzed three-component Michael addition/cyclization/cross-coupling reaction. *Angew. Chem., Int. Ed*. **2008**, *47*, 1903-1906. (f) Burns, D. J.; Best, D.; Wieczysty, M. D.; Lam, H. W. All-Carbon [3+3] Oxidative Annulations of 1,3-Enynes by Rhodium(III)-Catalyzed C-H Functionalization and 1,4-Migration. *Angew. Chem., Int. Ed.* **2015**, *54*, 9958−9962. (g) Huang, Y.; del Pozo, J.; Torker, S.; Hoveyda, A. H. Enantioselective Synthesis of Trisubstituted Allenyl−B(Pin) Compounds by Phosphine−Cu-Catalyzed 1,3-Enyne Hydroboration. Insights Regarding Stereochemical Integrity of Cu−Allenyl Intermediates. *J. Am. Chem. Soc*. **2018**, *140*, 2643-2655. (h) Ye, C.; Li, Y.; Zhu, X.; Hu, S.; Yuan, D.; Bao, H. Copper-Catalyzed 1,4-Alkylarylation of 1,3-Enynes with Masked Alkyl Electrophiles. *Chem. Sci*. **2019**, *10* (12), 3632−3636. (i) Zhu, X.; Deng, W.; Chiou, M.-F.; Ye, C.; Jian, W.; Zeng, Y.; Jiao, Y.; Ge, L.; Li, Y.; Zhang, X.; Bao, H. Copper-Catalyzed Radical 1,4-Difunctionalization of 1,3-Enynes Alkyl Diacyl Peroxides and N-Fluorobenzenesulfonimide. *J. Am. Chem. Soc*. **2019**, *141*, 548−559.

(6) For selected examples, see: (a) Choi, C. K.; Tomita, I.; Endo, T. Synthesis of Novel π-Conjugated Polymer Having an Enyne Unit by Palladium-Catalyzed Three-Component Coupling Polymerization and Subsequent Retro-Diels−Alder Reaction. *Macromolecules* **2000**, *33*, 1487-1488. (b) Campbell, K.; Kuehl, C. J.; Ferguson, M. J.; Stang, P. J.; Tykwinski, R. R. Coordination-driven self-assembly: solids with bidirectional porosity. *J. Am. Chem. Soc*. **2002**, *124*, 7266−7267. (c) Liu, Y.; Nishiura, M.; Wang, Y.; Hou, Z. M. π-Conjugated Aromatic Enynes as a Single-Emitting Component for White Electroluminescence. *J. Am. Chem. Soc*. **2006**, *128*, 5592−5593. (d) Pilzak, G. S.; Lagen, B. V.; Hendrikx, C. C. J.; Sudhölter, E. J. R.; Zuilhof, H. Synthesis and Optical Properties of all-trans-Oligodiacetylenes. *Chem. Eur. J*. **2008**, *14*, 7939−7950. (e) Cao, Z.; Ren, T. DFT Study of Electronic Properties of 3d Metal Complexes of σ-Geminal Diethynylethenes (gem-DEEs). *Organometallics*. **2011**, *30*, 245−250.

(7) For selected examples, see: (a) Sang, H. L.; Wu, C.; Phua, G. G. D.; Ge, S. Cobalt-Catalyzed Regiodivergent Stereoselective Hydroboration of 1,3-Diynes To Access Boryl-Functionalized Enynes. *ACS Catal*. **2019**, *9*, 10109−10114. (b) Liu, J.; Yang, J.; Schneider, C.; Frank, R.; Jackstell, R.; Beller, M. Tailored Palladium Catalysts for Selective Synthesis of Conjugated Enynes by Monocarbonylation of 1,3-Diynes. *Angew. Chem., Int. Ed*. **2020**, *59*, 9032−9040. (c) Cembellín, S.; Dalton, T.; Pinkert, T.; Schafers, F.; Glorius, F. Highly Selective Synthesis of 1,3-¨Enynes, Pyrroles, and Furans by Manganese(I)-Catalyzed C−H Activation. *ACS Catal*. **2020**, *10*, 197−202. (d) Liu, J.; Schneider, C.; Yang, J.; Wei, Z.; Jiao, H.; Franke, R.; Jackstell, R.; Beller, M. A General and Highly Selective Palladium-Catalyzed Hydroamidation of 1,3-Diynes. *Angew. Chem. Int. Ed*. **2021**, *133*, 375–383; (e) Sun, F.; Yang, C.; Ni, J.; Cheng, G.-J.; Fang, X. Ligand-Controlled Regiodivergent NickelCatalyzed Hydrocyanation of Silyl-Substituted 1,3-Diynes. *Org. Lett*. **2021**, *23*, 4045−4050.

(8) (a) Korotvicka, A.; Císarˇova´, I.; Roithova´, J.; Kotora, M. Synthesis of Aromatic Compounds by Catalytic C-C Bond Activation of Biphenylene or Angular [3] Phenylene. *Chem. - Eur. J.* **2012**, *18*, 4200−4207. (b) Gu, Z.; Boursalian, G. B.; Gandon, V.; Padilla, R.; Shen, H.; Timofeeva, T. V.; Tongwa, P.; Vollhardt, K. P. C.; Yakovenko, A. A. Activated Phenacenes from Phenylenes by Nickel-Catalyzed Alkyne Cycloadditions. *Angew. Chem., Int. Ed*. **2011**, *50*,

9413−9417. (c) Takano, H.; Kanyiva, K. S.; Shibata, T. Iridium-Catalyzed Formal [4 + 1] Cycloaddition of Biphenylenes with Alkenes Initiated by C-C Bond Cleavage for the Synthesis of 9,9-Disubstituted Fluorenes. *Org. Lett.* **2016**, *18*, 1860−1863. (d) Xu, Y.; Qi, X.; Zheng, P.; Berti, C. C.; Liu, P.; Dong, G. Deacylative transformations of ketones via aromatization-promoted C–C bond activation. *Nature*. **2019**, *567*, 373−378.

(9) (a) Fumagalli, G.; Stanton, S.; Bower, J. F. Recent Methodologies That Exploit C−C Single-Bond Cleavage of Strained Ring Systems by Transition Metal Complexes. *Chem. Rev*. **2017**, *117*, 9404−9432; (b) Biletskyi, B.; Colonna, P.; Mason, K.; Parrain, J.L.; Commeiras, L.; Chouraqui, G. Small rings in the bigger picture: ring expansion of three- and four-membered rings to access larger all-carbon cyclic systems. *Chem. Soc. Rev*. **2021**, *50*, 7513-7538.

(10) (a) Jun, C.-H.; Lee, H.; Moon, C. W.; Hong, H.-S. Cleavage of Carbon-Carbon Triple Bond of Alkyne via Hydro-iminoacylation by Rh (I) catalyst. *J. Am. Chem. Soc*. **2001**, *123*, 8600−8601. (b) Deng, L.; Chen, M.; Dong, G. Concise Synthesis of (−)-Cycloclavine and (−)-5-epi-Cycloclavine via Asymmetric C−C Activation. *J. Am. Chem. Soc.* **2018**, *140*, 9652−9658. (c) Ma, X. F.; Hazelden, I. R.; Langer, T.; Munday, R. H.; Bower, J. F. Enantioselective aza-heck cyclizations of N-(tosyloxy)carbamates: Synthesis of pyrrolidines and piperidines. J. *Am. Chem. Soc*. **2019**, *141*, 3356−3360. (d) Bruffaerts, J.; Vasseur, A.; Singh, S.; Masarwa, A.; Didier, D.; Oskar, L.; Perrin, L.; Eisenstein, O.; Marek, I. Zirconocene-Mediated Selective C-C Bond Cleavage of Strained Carbocycles: Scope and Mechanism. *J. Org. Chem.* **2018**, *83*, 3497−3515. (e) Jiao, L.; Yuan, C.; Yu, Z.-X. Tandem Rh (I)-Catalyzed [(5+2)+1] Cycloaddition/Aldol Reaction for the Construction of Linear Triquinane Skeleton: Total Syntheses of (±)-Hirsutene and (±)-1-Desoxyhypnophilin. *J. Am. Chem. Soc*. **2008**, *130*, 4421−4430. (f) Li, S.; Shi, P.; Liu, R.-H.; Hu, X.-H.; Loh, T.-P. Cobalt-Catalyzed N−O and C−C Bond Cleavage in 1,2-Oxazetidines: SolventControlled C−H Aminomethylation and Hydroxymethylation of Heteroarenes. *Org. Lett.* **2019**, *21*, 1602−1606.

(11) (a) Rosa, D.; Orellana, A. Palladium-catalyzed cross-coupling of cyclopropanol-derived ketone homoenolates with aryl bromides. *Chem. Commun*. **2013**, *49*, 5420-5422. (b) Parida, B. B.; Das, P. P.; Niocel, M.; Cha, J. K. C-Acylation of Cyclopropanols: Preparation of Functionalized 1,4-Diketones. *Org. Lett.* **2013**, *15*, 1780−1783. (c) Cheng, K.; Walsh, P. J. Arylation of Aldehyde Homoenolates with Aryl Bromides. *Org. Lett.* **2013**, *15*, 2298−2301. (d) Nithiy, N.; Orellana, A. Palladium-Catalyzed Cross-Coupling of Benzyl Chlorides with Cyclopropanol-Derived Ketone Homoenolates. *Org. Lett*. **2014**, *16*, 5854-585. (e) Liu, H.; Fu, Z.; Gao, S.; Huang, Y.; Lin, A.; Yao, H. Palladium-Catalyzed Hydroalkylation of Alkynes with Cyclopropanols: Access to γ,δ-Unsaturated Ketones. *Adv. Synth. Catal*. **2018**, *360*, 3171−3175. (f) Reding, A.; Jones, P. G.; Werz, D. B. Intramolecular trans Carbocarbonation of Internal Alkynes by a Cascade of Formal anti Carbopalladation/Cyclopropanol Opening. *Org. Lett*. **2018**, *20*, 7266−7269.

(12) (a) Ye, Z.; Dai, M. An Umpolung Strategy for the Synthesis of *β*-Aminoketones via Copper-Catalyzed Electrophilic Amination of Cyclopropanols. *Org. Lett*. **2015**, *17*, 2190−2193. (b) Ye, Z.; Gettys, K. E.; Shen, X.; Dai, M. Copper-Catalyzed Cyclopropanol Ring Opening Csp^3−Csp3 Cross-Couplings with (Fluoro)Alkyl Halides. *Org. Lett.* **2015**, *17*, 6074−6077. (c) Li, Y.; Ye, Z.; Bellman, T. M.; Chi, T.; Dai, M. Efficient Synthesis of *β*-CF_3/SCF_3-Substituted Carbonyls via Copper-Catalyzed Electrophilic Ring-Opening Cross-Coupling of Cyclopropanols. *Org. Lett*. **2015**, *17*, 2186−2189. (d) He, X.-P.; Shu, Y.-J.; Dai, J.-J.; Zhang, W.-M.; Feng, Y.-S.; Xu, H.-J. Copper-catalysed ring-opening trifluoromethylation of cyclopropanols. *Org. Biomol. Chem*. **2015**, *13*, 7159-7163. (e) Zhang, H.; Wu, G.; Yi, H.; Sun, T.; Wang, B.; Zhang, Y.; Dong, G.; Wang, J. Cu(I)-Catalyzed Chemoselective Coupling of Cyclopropanols with Diazo Esters: Ring-Opening C-C Bond Formations. *Angew. Chem., Int. Ed*. **2017**, *56*, 3945−3950. (f) Konik, Y. A.; Elek, G. Z.; Kaabel, S.; Jarving, I.; Lopp, M.;¨ Kananovich, D. G. Synthesis of *γ*-Keto Sulfones by Copper-Catalyzed Oxidative Sulfonylation of Tertiary Cyclopropanols. *Org. Biomol. Chem.* **2017**, *15*, 8334−8340. (g) Ye, Z.; Cai, X.; Li, J.; Dai, M. Catalytic cyclopropanol ring opening for divergent syntheses of *γ*-butyrolactones and *δ*-ketoesters containing all-carbon quaternary centers. *ACS Catal*. **2018**, *8*, 5907-5914; (h) Konik, Y. A.; Kudrjashova, M.; Konrad, N.; Kaabel, S.; Jarving, I.; Lopp, M.; Kananovich, D. G. Two-step conversion of carboxylic esters into distally fluorinated ketones via ring cleavage of cyclopropanol intermediates: application of sulfinate salts as fluoroalkylating reagents. *Org. Biomol. Chem*. **2017**, *15*, 4635−4643; (i) Gyanchander, E.; Ydhyam, S.; Tumma, N.; Belmore, K.; Cha, J. K. Mechanism of Ru(II)-Catalyzed Rearrangements of Allenyl- and Alkynylcyclopropanols to Cyclopentenones. *Org. Lett*. **2016**, *18*, 6098−6101 and references cited therein

(13) (a) Yang, J.; Shen, Y.; Lim, Y. J.; Yoshikai, N. Divergent ring opening coupling between cyclopropanols and alkynes under cobalt catalysis. *Chem. Sci*. **2018**, *9*, 6928−6934. (b) Yang, J.; Sun, Q.; Yoshikai, N. Cobalt-Catalyzed Regio- and Diastereoselective Formal [3 + 2] Cycloaddition between Cyclopropanols and Allenes. *ACS Catal*. **2019**, *9*, 1973−1978. (c) Yang, J.; Sekiguchi, Y.; Yoshikai, N. Cobalt-Catalyzed Enantioselective and Chemodivergent Addition of Cyclopropanols to Oxabicyclic Alkenes. *ACS Catal*. **2019**, *9*, 5638−5644; (d) Mills, L. R.; Zhou, C.; Fung, E.; Rousseaux, S. A. L. NiCatalyzed *β*-Alkylation of Cyclopropanol-Derived Homoenolates. *Org. Lett*. **2019**, *21*, 8805−8809. (e) J.-C. Li, Y. Zheng, M.-X. Huang and W.-F. Li, *Org. Lett.* **2020**, 22, 5020–5024. (f) Sekiguchi, Y.; Yoshikai, N. Enantioselective Conjugate Addition of Catalytically Generated Zinc Homoenolate. *J. Am. Chem. Soc*. **2021**, *143*, 4775−4781. (g) Huang, W.; Meng, F.-K. Cobalt-Catalyzed Diastereo- and Enantioselective Hydroalkylation of Cyclopropenes with Cobalt Homoenolates. *Angew. Chem., Int. Ed*. **2021**, *59*, 2694−2698.

(14) For selected examples, see: (a) Nanda, T.; Ravikumar, P. C. A Palladium-Catalyzed Cascade C− C Activation of Cyclopropenone and Carbonylative Amination: Easy Access to Highly Functionalized Maleimide Derivatives. *Org. Lett*. **2020**, *22*, 1368−1374. (b) Pati, B. V.; Ghosh, A.; Ravikumar, P. C. Rhodium-Catalyzed Room Temperature C−C Activation of Cyclopropanol for One-Step Access to Diverse 1,6-Diketones. *Org. Lett*. **2020**, *22*, 2854−2860. (c) Nanda, T.; Biswal, P.; Pati, B. V.; Banjare, S. K.; Ravikumar, P. C. Palladium Catalyzed C-C Bond Activation of Cyclopropenone: Modular Access to Trisubstituted α,β-Unsaturated Esters and Amides. *J. Org. Chem*. **2021**, *86*, 2682−2695.

(15) Lee, C.; Yang, W.; Parr, R. G. Development of the Colle-Salvetti correlation-energy formula into a functional of the electron density. *Phys. Rev. B.* **1980**, *37*, 785-789.

(16) Becke, A.D. A new mixing of Hartree–Fock and local density-functional theories. *J. Chem. Phys*. **1993**, *98*, 1372−1377.

(17) Clark, T.; Chandrasekhar, J.; Spitznagel, G. W.; Schleyer, P. V. R. Efficient diffuse function-augmented basis-sets for anion calculations. *J. Comput. Chem*. **1983**, *4*, 294−301.

(18) Wadt, W.R.; Hay, P.J. Ab initio effective core potentials for molecular calculations. Potentials for main group elements Na to Bi. *J. Chem. Phys*. **1985**, *82*, 284–298.

(19) Marenich, A.V.; Cramer, C.J.; Truhlar, D.G. Universal Solvation Model Based on Solute Electron Density and on a Continuum Model of the Solvent Defined by the Bulk Dielectric Constant and Atomic Surface Tensions. *J. Phys. Chem. B* **2009**, *113*, 6378–6396.

(20) Maes, B. U. W.; Verbeeck, S.; Verhelst, T.; Ekomie, A.; Von´ Wolff, N.; Lefevre, G.; Mitchell, E. A.; Jutand, A. Oxidative addition of` haloheteroarenes to palladium(0): Concerted versus SNAr-type mechanism. *Chem. - Eur. J*. **2015**, *21*, 7858−7865.

(21) Kozuch, S. A refinement of everyday thinking: the energetic span model for kinetic assessment of catalytic cycles. Wiley Interdiscip. Rev.: *Comput. Mol. Sci*. **2012**, *2*, 795–815.

Table of Contents